

The Mechanism of ATP-Dependent Primer-Template Recognition by a Clamp Loader Complex

Kyle R. Simonetta,¹ Steven L. Kazmirski,^{1,4} Eric R. Goedken,^{1,5} Aaron J. Cantor,¹ Brian A. Kelch,¹ Randall McNally,¹ Steven N. Seyedin,¹ Debora L. Makino,^{1,6} Mike O'Donnell,³ and John Kuriyan^{1,2,*}

¹Department of Molecular and Cell Biology, Department of Chemistry, Howard Hughes Medical Institute, University of California, Berkeley, Berkeley, CA 94720, USA

²Physical Biosciences Division, Lawrence Berkeley National Laboratory, Berkeley, CA 94720, USA

³Howard Hughes Medical Institute, Rockefeller University, 1230 York Avenue, Box 228, New York, NY 10021, USA

⁴Present address: AstraZeneca R&D Boston, 35 Gatehouse Drive, Waltham, MA 02451, USA

⁵Present address: Abbott Bioresearch Center, 100 Research Drive, Worcester, MA 01605, USA

⁶Present address: Max Planck Institute of Biochemistry, Department of Structural Cell Biology, Am Klopferspitz 18, D-82152 Martinsried, Germany

*Correspondence: kuriyan@berkeley.edu

DOI 10.1016/j.cell.2009.03.044

SUMMARY

Clamp loaders load sliding clamps onto primer-template DNA. The structure of the *E. coli* clamp loader bound to DNA reveals the formation of an ATP-dependent spiral of ATPase domains that tracks only the template strand, allowing recognition of both RNA and DNA primers. Unlike hexameric helicases, in which DNA translocation requires distinct conformations of the ATPase domains, the clamp loader spiral is symmetric and is set up to trigger release upon DNA recognition. Specificity for primed DNA arises from blockage of the end of the primer and accommodation of the emerging template along a surface groove. A related structure reveals how the ψ protein, essential for coupling the clamp loader to single-stranded DNA-binding protein (SSB), binds to the clamp loader. By stabilizing a conformation of the clamp loader that is consistent with the ATPase spiral observed upon DNA binding, ψ binding promotes the clamp-loading activity of the complex.

INTRODUCTION

High-speed DNA replication relies on the anchorage of DNA polymerases to sliding DNA clamps, known as the β clamp in bacteria, PCNA in eukaryotes and archaea, and gp45 in bacteriophage T4 (Bowman et al., 2005). Sliding clamps are loaded onto DNA by a pentameric ATP-dependent complex known as the clamp loader (Johnson and O'Donnell, 2005). Along with hexameric helicases and DNA translocases, the clamp loaders are oligomeric ATPases that use similar structural elements to recognize DNA or RNA helices, which take a position analogous to that of the central shaft in the F_1 -ATPase assembly (Abrahams et al., 1994; Enemark and Joshua-Tor, 2006; Skordalakes and Berger, 2006).

Whereas helicases and translocases use ATP hydrolysis to power movement, the clamp loaders use ATP hydrolysis to trigger release of the ATPase from DNA (Pietroni and von Hippel, 2008).

The subunits of bacterial clamp loaders are related to those of the eukaryotic and archaeobacterial clamp loaders (replication factor C, RFC) and the gp44/62 complex in bacteriophage T4 (Benkovic et al., 2001; Bowman et al., 2004; Cullmann et al., 1995; Guenther et al., 1997; Kelman and White, 2005; O'Donnell et al., 1993; Oyama et al., 2001). The two N-terminal domains (domains 1 and 2) of each clamp loader subunit form an AAA+ ATPase module (ATPases associated with a variety of cellular activities) (Figure 1A), and the C-terminal domain (domain 3) is integrated into a circular collar (Jeruzalmi et al., 2001a; Neuwald et al., 1999). The bacterial clamp loader, known as the γ/τ complex (referred to here as the γ complex), contains three copies of the γ subunit, which is an active ATPase, and one copy each of the structurally related δ and δ' subunits, which have degenerate ATP-binding sites (Figure 1A). ATP binding to the clamp loader leads to stable interaction with an open sliding clamp (Figure 1A) (Hingorani and O'Donnell, 1998; Jeruzalmi et al., 2001b; Naktinis et al., 1995). The ATPase activity of the clamp loader is stimulated by the binding of primer-template DNA, i.e., a double-strand/single-strand junction with a 5' overhang (Ason et al., 2003). ATP hydrolysis results in the release of the closed clamp around DNA (Pietroni and von Hippel, 2008; Zhuang et al., 2006a, 2006b).

A breakthrough in our understanding of clamp loader function occurred with the determination of the structure of an ATP-loaded state of the yeast RFC complex bound to the PCNA sliding clamp obtained in the absence of DNA (Bowman et al., 2004). This structure evoked a "notched screw cap" model for recognition of primer-template DNA by the clamp loader. ATP binding was proposed to induce an observed spiral arrangement of ATPase subunits, which "screws" onto double-helical DNA. The clamp loader subunits are so arranged that if they were to track the minor groove, then the 3' end of the primer strand would run into the interior of the central chamber, whereas the

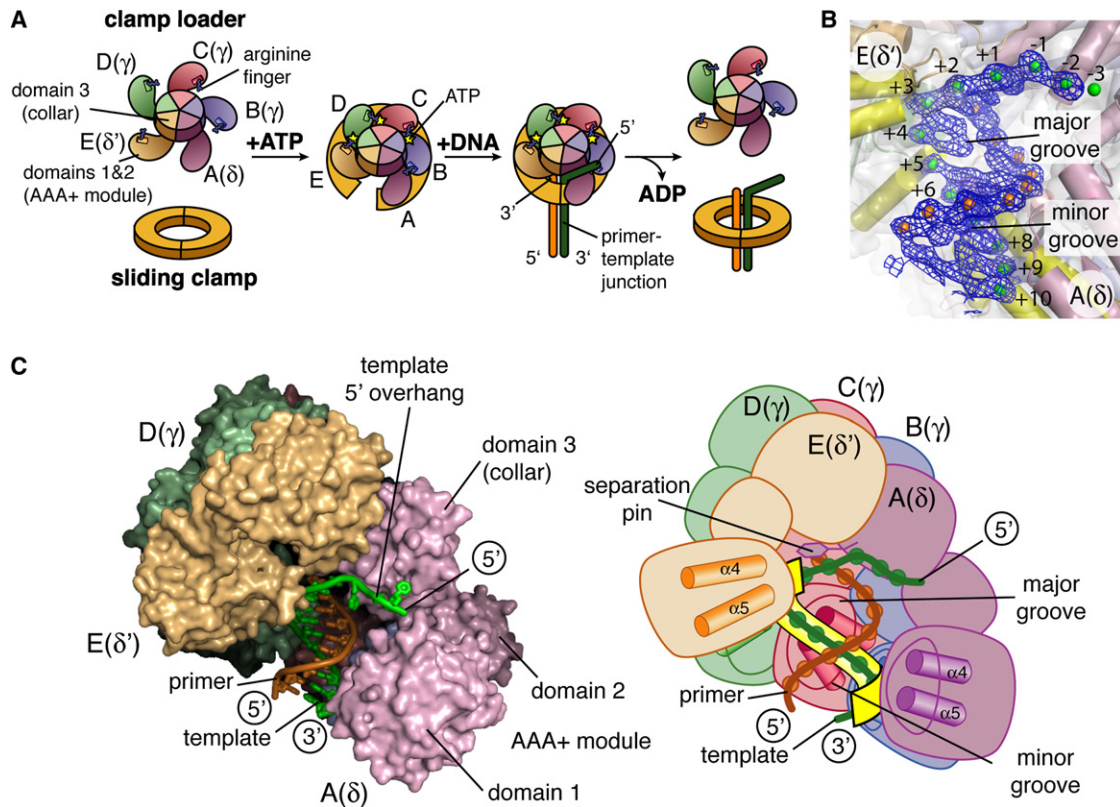


Figure 1. Structure of the Clamp Loader:DNA Complex

(A) Schematic diagram of the clamp loader cycle.

(B) Unbiased electron density for the DNA, calculated using a model at a stage prior to the inclusion of DNA and improved using density modification (Terwilliger, 2000). Contour lines at 1.2 SD above the mean are shown in blue. The phosphate groups in the final DNA model are shown as spheres. The DNA-interacting helices of the clamp loader are shown in yellow in this and subsequent figures.

(C) The structure of wild-type γ complex bound to primer-template DNA (left) and a schematic representation (right). The contacts between the clamp loader and the template strand are restricted primarily to the template strand, which is shown outlined in yellow.

extended template strand would end up aligned with a gap in the clamp loader assembly.

Although the RFC:PCNA structure led to a compelling model for the binding of DNA by clamp loader complexes, there is little direct evidence that the essential features of this model are correct. That DNA does indeed bind within the central chamber of the clamp loaders has been confirmed by mutagenesis and electron microscopy (Goedken et al., 2005; Miyata et al., 2005; Yao et al., 2006). Both single-stranded and double-stranded DNA can form helices with similar rise and pitch, and, therefore, the spiral arrangement of ATPase subunits does not by itself establish what form of DNA is recognized. This ambiguity is highlighted by the crystal structure of the DNA complex of E1 helicase from papillomavirus in which the AAA+ modules spiral around helical single-stranded DNA (Enemark and Joshua-Tor, 2006). The RFC:PCNA complex was crystallized using mutant RFC subunits in which each of the interfacial "arginine finger" residues was replaced by glutamine (Bowman et al., 2004). Perhaps as a consequence of these mutations, the relationship between AAA+ modules in the spiral is not uniform, resulting in alternating tight and loose ATP-binding sites and a central chamber that is too small for a double helix.

It is also unclear how the clamp loader recognizes both DNA and RNA primers. The *E. coli* clamp loader loads sliding clamps onto templates primed with RNA during replication but can also utilize DNA primers during the repair of damaged DNA (Lahue et al., 1989). In eukaryotes, the RNA primer is extended by a DNA polymerase to form a DNA:DNA primer-template junction that is recognized by the RFC clamp loader complex (Waga and Stillman, 1998). The RFC complex does, however, retain the ability to load sliding clamps onto DNA templates primed with RNA (Yuzhakov et al., 1999).

A critical aspect of high-speed DNA replication is the interaction of single-stranded DNA, located upstream of newly synthesized Okazaki fragments, with single-stranded DNA-binding protein (SSB). Bacterial clamp loaders are physically linked to SSB by a heterodimer of two proteins (χ and ψ), and this linkage increases replication activity (Glover and McHenry, 1998; Kelman et al., 1998). The ψ protein binds tightly to the collar domain of the γ subunits of the clamp loader (Olson et al., 1995). The χ protein docks on to the C-terminal tail segment of SSB, thus bridging the clamp loader and SSB (Kelman et al., 1998; Witte et al., 2003). The presence of ψ is not essential for clamp loader activity, but it potentiates binding to the sliding clamp and DNA

and stimulates DNA-dependent ATP hydrolysis (Anderson et al., 2007). The mechanism underlying this stimulation of clamp loader activity by the ψ protein is not understood.

We now present the crystal structure of the *E. coli* clamp loader complex bound to primer-template DNA and to a segment of the ψ protein. The structure of the DNA complex reveals that the notched screw cap model for primer-template recognition is correct in its essential features (Bowman et al., 2004). The structure reveals a highly symmetrical arrangement of ATPase subunits that matches the conformation of DNA and the 6-fold pseudosymmetry of the sliding clamp. Each of the ATP-binding sites appears primed for catalysis, suggesting that DNA recognition generates a “suicide complex” in which ATP hydrolysis triggers conversion to an inactive conformation in which the spiral organization is broken (Jeruzalmi et al., 2001a). An unanticipated aspect of the structure is that contacts between the protein and DNA are restricted primarily to the template strand, which explains how clamp loaders can accommodate both RNA and DNA primers. We also show that ψ binding breaks a symmetry in the collar domain that arises from the presence of three identical copies of the γ subunit within the complex. The domains that form the collar switch to a less symmetrical conformation upon DNA binding, which is the conformation that is recognized by the ψ protein.

RESULTS AND DISCUSSION

Structure Determination

The wild-type *E. coli* clamp loader complex was crystallized with the ATP analog ADP•BeF₃ and primer-template DNA containing a duplex segment of 10 base pairs and a 5 nucleotide 5' overhang. The structure was determined at a resolution of 3.4 Å (Tables S1 and S4 available online). The asymmetric unit in the crystal contains two clamp loader complexes. Isomorphous crystals were also obtained using a mutant form of the γ subunit in which a threonine side chain at the active site (Thr 157) was replaced with alanine. This mutation prevents ATP hydrolysis (Hattendorf and Lindquist, 2002). Crystals of this variant γ complex bound to ADP•BeF₃ and a primer-template junction with a 10 base pair duplex segment and a 10 nucleotide overhang diffracted X-rays to 3.25 Å resolution (Table S2). There are no apparent differences in structure between the wild-type and mutant complexes. We restrict discussion to the wild-type complex, and the data for the mutant complex were used to verify our analysis.

Preliminary electron density maps allowed unambiguous visualization of the ADP•BeF₃ molecules bound to the three γ subunits, as well as the entire primer-template DNA bound to each complex, except for the last three nucleotides in the overhang (Figure 1B). Electron density for the clamp loader subunits is also strong throughout both complexes. As a consequence, the features of the structure (Figure 1C) on which we base our analysis are determined reliably.

DNA Recognition by the Clamp Loader Complex

The AAA+ modules of the B, C, D, and E subunits form a right-handed spiral around the double-stranded portion of the DNA, which is in a slightly distorted B-form conformation (Figures 1C

and 2A). Domain 1 of the A(δ) subunit is disengaged from DNA (Figure S1). The corresponding subunit in the RFC:PCNA complex is fully integrated into the clamp loader spiral and provides the primary contact with the clamp (Bowman et al., 2004). Therefore, it seems likely that the absence of the clamp in the γ complex structure accounts for the disengagement of the A subunit from the ATPase spiral.

At first glance, the structure of the DNA complex looks strikingly like that predicted on the basis of the RFC:PCNA model (Bowman et al., 2004) and visualized at low resolution in electron microscopic reconstructions (Miyata et al., 2005). But closer examination shows an unanticipated feature, which is that the recognition of DNA is mediated primarily by interactions with phosphate groups in the template strand alone (Figure 2). The primer strand does not make close contact with the clamp loader, with the exception of the 3' terminal nucleotide. Hexameric helicases encircle one strand of DNA (Enemark and Joshua-Tor, 2006), and the clamp loader can be thought of as a helicase that has “lost” one subunit. The lack of the sixth subunit allows the primer strand in the duplex to be accommodated—but without tight contact—and provides an exit channel for the template.

The AAA+ domains of the B, C, D, and E subunits track the template strand in dinucleotide steps (Figure 2A), and the interactions made by these subunits are consistent with the effects of mutations in the clamp loader (Figures 2B and 2C) (Goedken et al., 2005). The positive ends of the helix dipoles of helices α 4 and α 5 within each subunit are positioned close to negatively charged phosphate groups, and the tips of these two helices are bisected by the backbone of the template strand (see the D(γ) subunit in Figure 2A).

An important interaction with the primer strand occurs at the very end of the duplex segment. The collar domain of the A(δ) subunit positions the side chain of Tyr 316 so that it stacks on the nucleotide base at the 3' end of the primer strand (Figure 2D). This results in termination of the primer strand and a sharp bend in the template strand as it exits the clamp loader chamber. The blocking function of the Tyr 316 side chain is reminiscent of the role of an aromatic side chain in the UvrD helicase that serves as a “separation pin” by splitting the path of DNA (Lee and Yang, 2006).

DNA Induces a Highly Symmetrical Arrangement of AAA+ Modules that Appears to Promote Catalysis

The B, C, D, and E subunits are related to one another by a uniform rise and rotation around a common helical axis (Figures 2A and 3A). The three rotation axes are nearly coincident and run through the center of the clamp loader chamber and also through the DNA. The C, D, and E subunits are each related to the preceding subunits by a rotation of $\sim 60^\circ$ and a rise of ~ 7.3 Å (58.8° and 7.4 Å, 59.1° and 7.2 Å, and 56.5° and 7.3 Å for the B-to-C, C-to-D, and D-to-E transformations, respectively). The corresponding values for dinucleotide steps in ideal B-form DNA are $\sim 72^\circ$ and ~ 6.8 Å, and the interactions with the clamp loader result in the DNA being slightly underwound. The rotational symmetry of the clamp loader subunits is a result of a near identical packing of adjacent subunits along the spiral (one of these interfaces is shown in Figure 3B). An alignment of

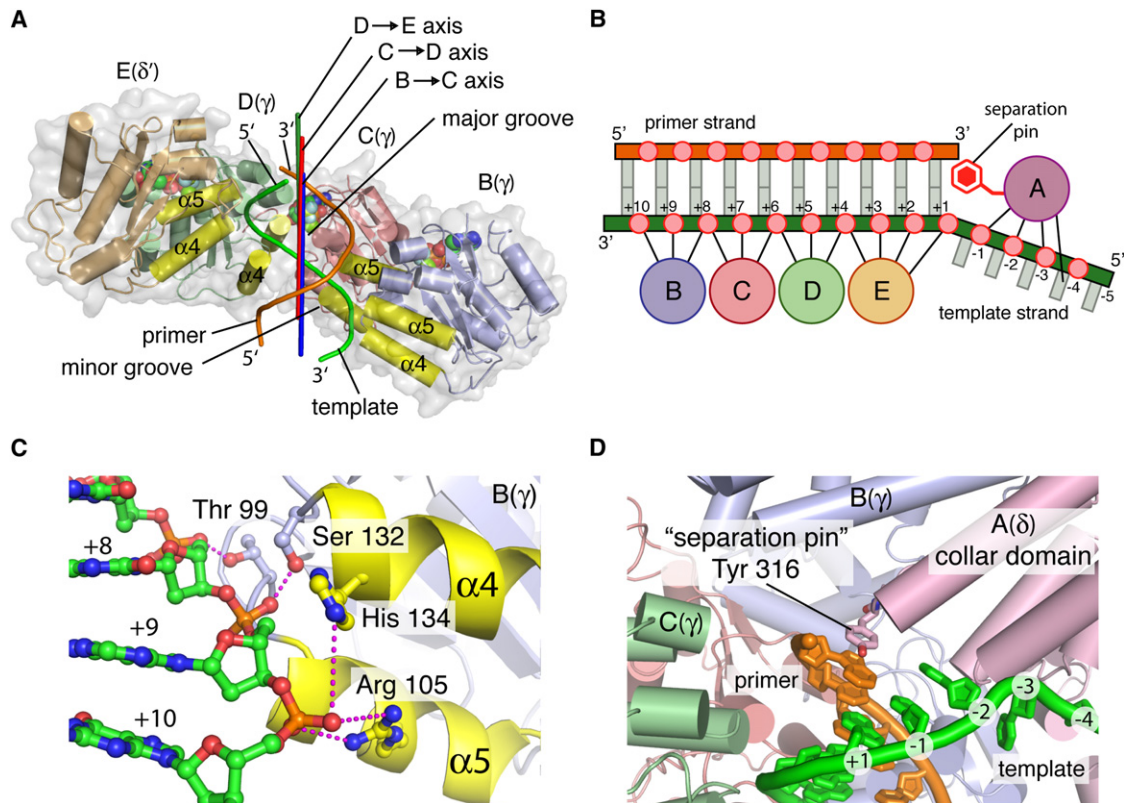


Figure 2. DNA Recognition

(A) Diagram showing the ATPase subunits of the clamp loader and DNA duplex. The DNA-interacting helices are shown in yellow. The three rotation axes that relate the B subunit to the C subunit, the C subunit to the D subunit, and the D subunit to the E subunit are shown in blue, red, and green, respectively. The three axes are nearly coincident with each other and with the axis of the DNA duplex (not shown).

(B) Schematic diagram of contacts with the primer-template DNA.

(C) Expanded view of a domain 1:DNA interaction, highlighting hydrogen-bonding interactions between the DNA and the protein.

(D) The side chain of Tyr 316 blocks the path of the primer strand by stacking on the last nucleotide base of the primer.

the three interfaces reveals that the protein subunits, as well as the phosphate groups of the template strand, overlay almost perfectly (Figure S2). A key interaction at each interface is the coordination of the BeF_3 moiety of the ATP analog by the arginine finger (e.g., Arg 169 in γ). This arginine is presented by an α helix, denoted the SRC helix because of a conserved sequence motif.

The symmetry in the quaternary arrangements of the ATPase domains of the γ complex results in the configuration of each interfacial ATP-binding site being essentially the same (Figure S3) and very similar to that of the two tighter ATP-binding sites in the RFC:PCNA structure (the A and C sites; Figure 3C) (Bowman et al., 2004). These sites in RFC were proposed to represent a catalytically competent conformation based on structural similarities with the ATP-binding interfaces in F_1 -ATPase (Bowman et al., 2004). We conclude, therefore, that all three of the ATP-binding interfaces in the structure of the γ complex bound to DNA are in a conformation that is also likely to be competent for ATP hydrolysis.

The location of ATP at the centers of symmetrically arranged interfaces suggests that ATP binding is highly cooperative and that DNA binding will promote catalysis (Gomes and Burgers, 2001; Gomes et al., 2001). The hydrolysis of a single ATP molecule

is likely to weaken the network of interactions that maintains the protein complex on DNA, consistent with biochemical analysis (Pietroni and von Hippel, 2008). The structure of the inactive form of the γ complex suggests that the loss of ATP will result in disengagement from the sliding clamp and completion of the clamp loader cycle (Jeruzalmi et al., 2001a; Kazmirski et al., 2004).

Comparison of the structures of the γ complex and the RFC:PCNA complex also suggests that the complete coordination of ATP results in a clamp loader conformation with increased complementarity to the surface of the sliding clamp. Analysis of this feature is based on the RFC:PCNA structure. We began with the structure of the RFC:PCNA complex in which the A subunit is docked onto PCNA and generated a model in which the transformation that relates the A subunit to the B subunit is applied, in turn, to the ATPase domains of the B, C, D, and E subunits. This results in a symmetric spiral arrangement of the RFC subunits above the PCNA clamp, which overlays closely with the structure of the γ complex (except for A(δ)). A striking feature of this model, seen in projection, is the improved alignment between the RFC subunits and five of the six pseudosymmetric domains of PCNA (Figure 3A, middle), compared to the crystal structure of the RFC mutant bound to PCNA (Figure 3A, right).

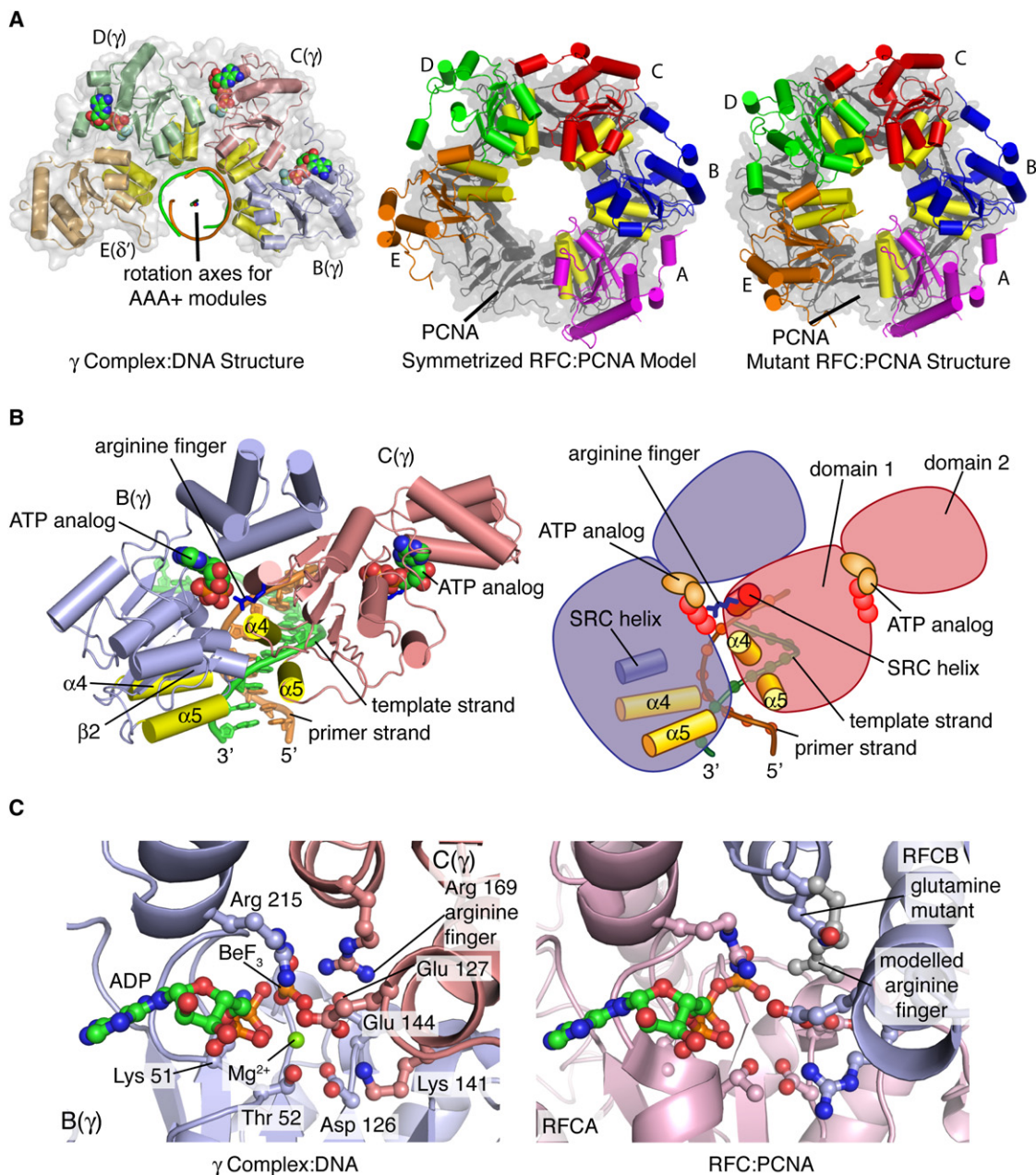


Figure 3. Symmetry in the AAA+ Spiral and Interfacial ATP Coordination

(A) (Left) The B, C, D, and E subunits (domain 1 only) of the γ complex, shown in a view that is orthogonal to that shown in Figure 2A. (Middle) A symmetrized version of the RFC clamp loader. In this model, the A subunit is in the same position, docked on the PCNA clamp, as in the crystal structure of the mutant RFC:PCNA complex (Bowman et al., 2004). The B, C, D, and E subunits are positioned by applying the transformation that relates one subunit to the next one in the γ complex. (Right) The actual positions of the RFC subunits in the crystal structure of the mutant RFC:PCNA complex.

(B) Coordination of the ATP analog bound to the B subunit by the arginine finger presented by the C subunit. Only the AAA+ modules (domains 1 and 2) are shown (left). A schematic representation of this interaction is also shown (right).

(C) An expanded view of the coordination of ADP•BeF₃ bound to B(γ) is shown on the left. A similar view of ATP γ S bound to the A subunit of the mutant RFC complex is shown on the right (Bowman et al., 2004). The arginine finger in each of the subunits of the mutant RFC complex is replaced by glutamine. A modeled arginine side chain at the glutamine position is shown in gray, and it is positioned to coordinate the γ phosphate of ATP, as do the actual arginine fingers in the γ complex. Each of the ATP-binding sites in the γ complex has essentially the same configuration of side chains shown here (see Figure S3). This symmetry is absent in the structure of the mutant RFC complex, in which only the A and C sites display tight coordination of ATP.

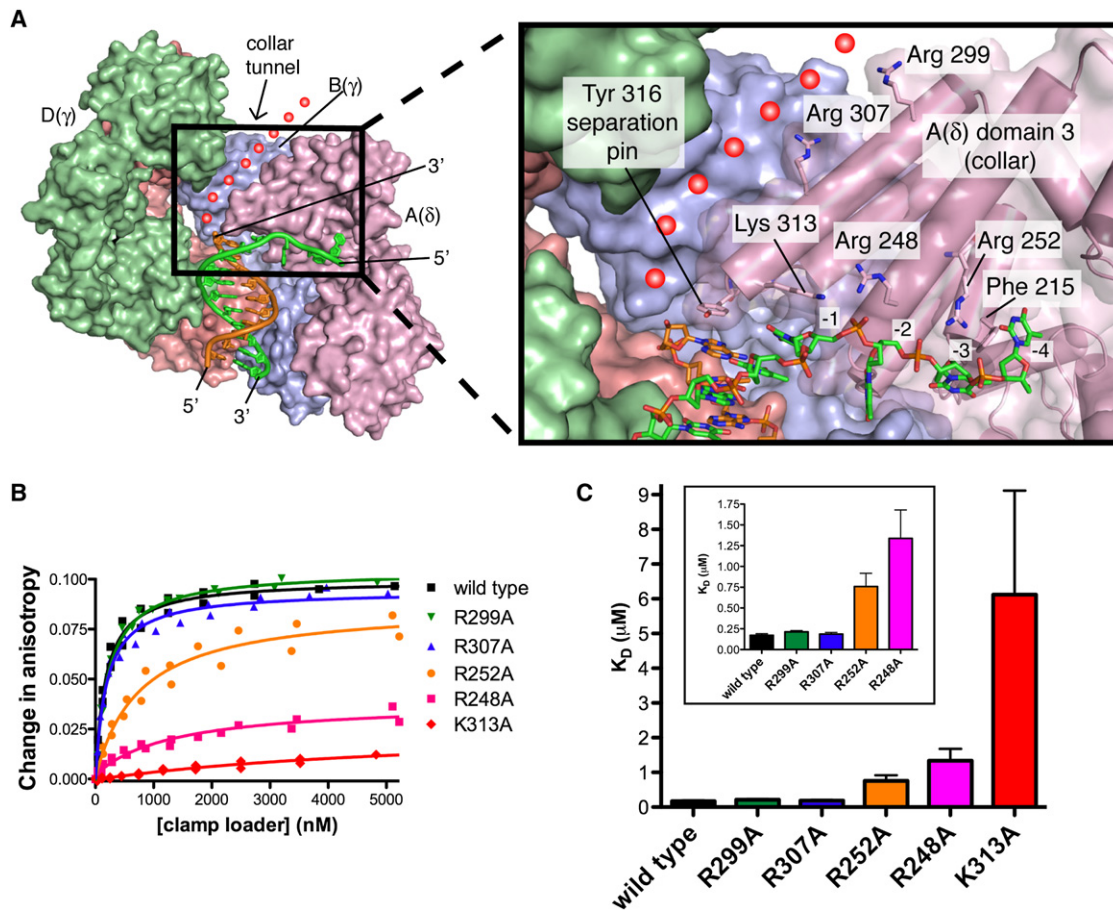


Figure 4. The Exit Channel for the Template Strand Overhang

(A) The structure of the clamp loader is shown, with the E(δ') subunit removed to reveal a tunnel leading through the collar, indicated by red spheres. In the expanded view on the right, side chains presented by the collar domain of the A(δ) subunit and that interact with DNA are shown. Two side chains that line the collar tunnel are also shown.

(B) Fluorescence anisotropy data for fluorescently labeled primer-template DNA binding to the wild-type γ complex and five mutants, in the presence of 1 μM β clamp, are shown. Mutation of residues that line the collar tunnel (R299A and R307A; see [A]) does not affect DNA-binding affinity, whereas mutation of residues that are in the observed exit path (R252A, R248A, and K313A) reduces DNA binding affinity.

(C) Dissociation constants of mutant clamp loaders for DNA. The inset shows a zoomed-in region of the chart. Error bars represent the SE of the fit.

The PCNA ring in this model is closed and flat, and it is unclear at present how ATP binding promotes interaction with an open form of the clamp. Analysis of the bacteriophage T4 clamp loader has shown that the open form of the clamp, in the absence of DNA, is most likely recognized by a form of the clamp loader in which the ATP-binding sites are not equivalent (Pietroni and von Hippel, 2008). There are no crystal structures available at present for an intact clamp loader bound to an open clamp, although a low-resolution view of such a complex has been obtained by electron microscopy (Miyata et al., 2005).

The Exit Channel for Single-Stranded DNA

The single-stranded 5' overhang of the template strand exits the central chamber of the clamp loader and binds to the exterior surface of the collar domain of A(δ), consistent with previous studies (Figure 4A) (Chen et al., 2008; Magdalena Coman et al., 2004). Mutation of residues located within the exit channel seen in the crystal structure has a drastic effect on the value of

the dissociation constant (K_D) for DNA binding (Figures 4B and 4C). Mutation of Lys 313 and Arg 248, which interact with the phosphate group of the nucleotide at the -1 position, increases the value of K_D from 0.18 ± 0.02 μM for wild-type protein to 6.1 ± 3.0 μM and 1.3 ± 0.3 μM for the mutants, respectively. Mutation of Arg 252, which interacts with the phosphate group of the nucleotide at the -2 position in the overhang, had a smaller effect ($K_D = 0.76 \pm 0.16$ μM). Mutation of residues in the exit channel also compromises the ability of the clamp loader to load clamps onto DNA (Figure S4).

The collar domains encircle a tunnel that leads into the site within the central chamber where the last nucleotide in the primer strand is bound (Figure 4A). Replacement of residues within the collar tunnel (e.g., Arg 299 and Arg 307) by alanine had no effect on primer-template DNA binding by the clamp loader or on DNA-induced clamp closing, indicating that the 5' overhang in a normal primer-template junction does not pass through this region (Figures 4B, 4C, and S4).

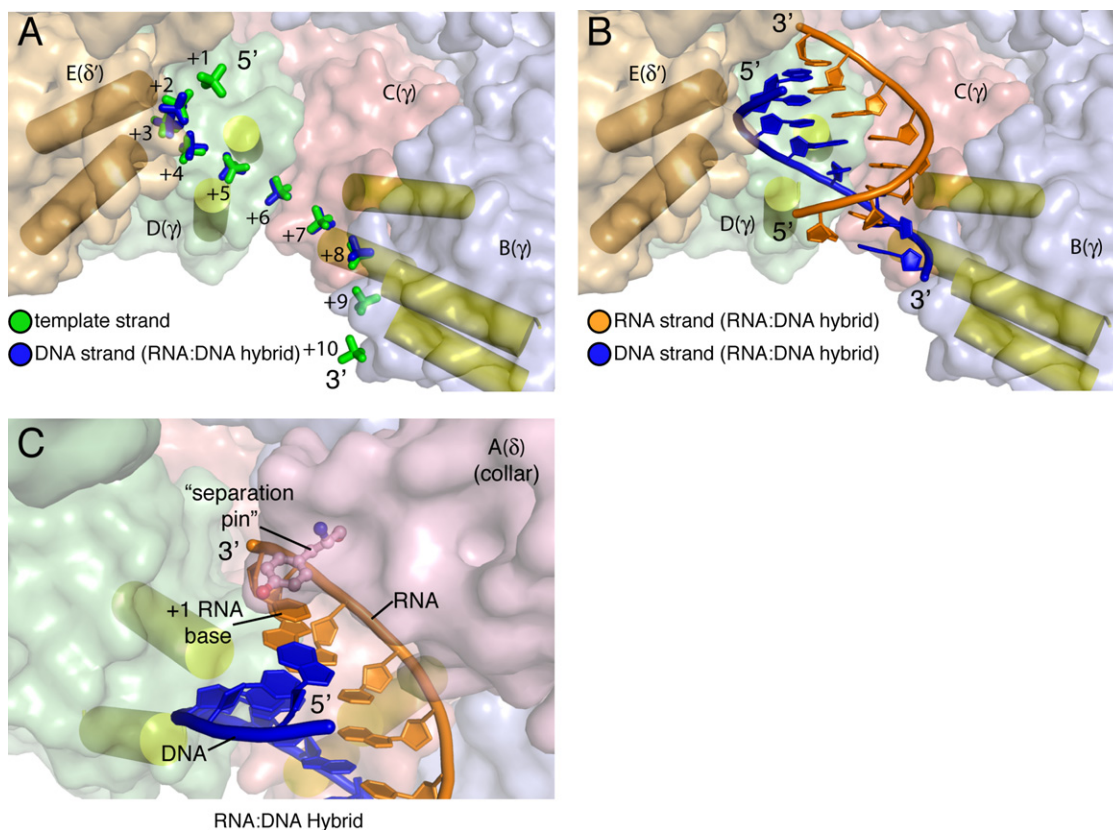


Figure 5. Recognition of RNA-DNA Hybrids

(A) The DNA strand of an RNA:DNA hybrid (Fedoroff et al., 1993; PDB code 124D) is aligned on the template strand in the crystal structure of the clamp loader. (B) The RNA and DNA strands of an RNA:DNA hybrid, aligned as in (A) are shown. The RNA strand (orange) is accommodated without steric clash because the clamp loader only engages the template strand. (C) The structure of an RNA:DNA hybrid, with its DNA strand aligned on the template strand in the crystal structure as in (A) and (B), is shown. Note that the RNA strand of the aligned hybrid duplex preserves the interaction with the separation pin (compare with Figure 2D).

The Clamp Loader Structure Is Consistent with the Recognition of RNA Primers

Alignment of the DNA strands of RNA:DNA hybrids (see, for example, Fedoroff et al., 1993 and Nowotny et al., 2005) with the template strand in our crystal structure reveals close overlap of the phosphate groups (Figure 5A). Over a 7 nucleotide stretch, the phosphate groups of the DNA strand in the hybrid duplex structure of Fedoroff et al. (1993) can be aligned onto the clamp loader template strand with an rmsd of 1.0 Å (the length of the alignment is limited by the length of the duplex in the hybrid structure). In contrast, the conformation of the modeled RNA strand diverges considerably from the structure of the DNA primer strand in the clamp loader complex. Nevertheless, because the primer strand is disengaged and mainly in a surface-exposed location, variation in the conformation of the primer can be accommodated. The phosphate backbone of the modeled RNA strand does not clash with the clamp loader and is located near the generally positive electrostatic environment of the central chamber (Figure 5B).

One important result of aligning the hybrid structures onto the template strand is that the terminal 3' base of the RNA strand in the docked hybrid structures ends up in essentially the same

location as the 3' base of the primer strand in the crystal structure. Thus, the "separation pin" (Tyr 316 in A(δ)) is positioned to make a stacking interaction with the nucleotide base at the 3' end of the primer strand, regardless of whether the primer is RNA or DNA (compare Figures 2D and 5C).

Clamp loaders involved in DNA damage repair in eukaryotes are formed by replacing a single subunit in the RFC complex with an alternate clamp loader subunit (the alternate subunit is Rad24 in yeast and Rad17 in humans and is located at the A position of the complex). This variant clamp loader loads a specialized clamp, the 9-1-1 complex, onto DNA with 3' overhangs, as opposed to the primer-template junctions with 5' overhangs that are recognized by the replicative clamp loaders (Ellison and Stillman, 2003). The restriction of contacts to the template strand also suggests a potential mechanism by which the specificity of a clamp loader might be switched by replacing the A subunit and by rotating the DNA, as discussed further in Supplemental Data.

Binding of the ψ Protein to the Clamp Loader

A 28 residue N-terminal segment of ψ has been identified as the region likely to anchor the χ : ψ heterodimer to the clamp loader

(Gulbis et al., 2004; Ozawa et al., 2005). The value of K_D for the interaction between the χ : ψ heterodimer and the clamp loader is ~ 10 nM (Gao and McHenry, 2001). We measured the affinity of a peptide spanning residues 2 to 28 of the N-terminal segment of ψ (referred to as the ψ peptide; this peptide does not include the first residue of ψ , which is not conserved) for the clamp loader using isothermal titration calorimetry. The ψ peptide binds to the clamp loader complex with a 1:1 stoichiometry, with a K_D value (7 nM) that is essentially the same as for the intact χ : ψ heterodimer (Figure 6A). The intact ψ protein potentiates DNA binding by the clamp loader (Anderson et al., 2007), and the isolated ψ peptide has a similar effect, in that it increases the affinity of the clamp loader complex for primer-template DNA by ~ 20 -fold (Figure 6B). These results indicate that the functional aspects of the interaction of ψ with the clamp loader are captured by the ψ peptide.

We determined the structure of the ψ peptide bound to the clamp loader in the presence of DNA at 3.5 Å resolution (Figure 6C, see Experimental Procedures). Despite the moderate resolution, electron density for the peptide is strong, consistent with tight binding. The presence of bulky tryptophan side chains at positions 7 and 17 allowed unambiguous determination of the register of the sequence of the peptide with the electron density (Figure S5). Interaction between the ψ peptide and the clamp loader is restricted to the collar domains of the three γ subunits, consistent with biochemical data and sequence conservation in the clamp loaders (Gao and McHenry, 2001; Gulbis et al., 2004) and also with the suggestion that ψ may facilitate the assembly of clamp loader complexes by stabilizing a trimer of γ subunits for interaction with the δ and δ' subunits (Gao and McHenry, 2001).

Residues 3 to 13 of the ψ peptide form an α helix that packs against the helices of the D(γ) and C(γ) subunits that line the inner surface of the collar (Figure 6D). The docking of the α helix is stabilized by residues that are highly conserved in ψ . Residues 14 to 19 of the ψ peptide form a β strand that runs along the surface of the C(γ) subunit and into the interface between the C(γ) and B(γ) subunits, forming a short two-stranded antiparallel β sheet with the C-terminal tail of the B(γ) subunit. Trp 17, which is invariant in ψ sequences, packs between the side chains of Pro 361 and Arg 355 of the B(γ) subunit of the clamp loader. A variant peptide containing Trp 17 replaced with serine binds to the clamp loader with 55-fold lower affinity, confirming the importance of this interaction (Figure 6A).

The ψ Peptide Breaks a Symmetry in the Collar Domain and Thereby Facilitates DNA Binding

In the absence of DNA, the *E. coli* clamp loader is in an inactive conformation in which the nucleotide-binding domains do not adopt the spiral arrangement seen in the DNA-bound form (Bowman et al., 2004; Jeruzalmi et al., 2001a; Kazmirski et al., 2004). Comparison with the structure of the DNA complex reveals that DNA binding is accompanied by a conformational change in the collar domain, localized to a rigid body rotation of the B(γ) subunit by $\sim 10^\circ$ with respect to the rest of the collar (Figure 7A).

The collar domains of the three identical γ subunits in the clamp loader are arranged symmetrically with respect to each other in the absence of DNA (Figure S6). In contrast, in the DNA complex, the rotation of the B(γ) domain breaks this natural

symmetry in the collar. The structure of the collar domain in the complex with ψ and DNA is essentially the same as that seen in the DNA complex without ψ , except for a localized rearrangement of the C-terminal tail of the B(γ) subunit, which forms a β sheet with the ψ peptide. The rotation in the collar domain of the B(γ) subunit is required for the interaction with ψ (Figure S6). Analysis of the structure of the ψ peptide cocrystallized with the clamp loader in the absence of DNA and nucleotide (see Supplemental Data) demonstrates that both DNA and ψ induce the same conformational change in the collar domain of the B(γ) subunit independently.

The collar domains of the clamp loader form a circle with rotational pseudosymmetry, which is inconsistent with the helical symmetry of the AAA+ modules when DNA is engaged. This symmetry mismatch is accommodated by differences in the orientation of the individual AAA+ modules with respect to the collar domains. In particular, the C(γ) and D(γ) subunits are in an extended conformation, whereas, in the B(γ) subunit, the AAA+ module rises up toward the collar domains (Figure 7B). The connection between the AAA+ module and the collar of the B(γ) subunit involves a tight junction between the last helix in the AAA+ module and the first helix in the collar domain, in contrast to the extended and looser connection seen in the C(γ) and D(γ) subunits. This junction can only form if the collar domain in the B(γ) subunit rotates downward to meet the AAA+ module, as seen in the DNA and ψ complexes.

The clamp loader complex from the bacterium *Pseudomonas aeruginosa* is divergent in sequence with respect to the *E. coli* clamp loader but is also activated by the corresponding χ : ψ heterodimer (Jarvis et al., 2005b). Intriguingly, the *E. coli* χ : ψ heterodimer can activate the *P. aeruginosa* clamp loader (Jarvis et al., 2005a). The N-terminal segments of the *E. coli* and *P. aeruginosa* ψ proteins are similar in sequence, and we assume that both ψ proteins act by breaking a symmetry in the collar domain that is naturally present in bacterial clamp loaders due to the use of three identical γ subunits.

Implications for Docking to SSB

Residues 20 to 28 of the ψ peptide fold over the upper rim of the collar domain at the interface between the C(γ) and B(γ), emerging at the outer surface of the clamp loader. This region of the ψ peptide is anchored by Leu 25, which is highly conserved. Residue 29 is an integral part of the folded structure of the ψ subunit in the χ : ψ heterodimer (Gulbis et al., 2004), thereby locating the χ : ψ heterodimer at the outer surface of the collar domain of the clamp loader, near the interface between the B and C subunits (see Figure 7C).

The structure of an SSB tetramer bound to DNA has been determined (Raghunathan et al., 2000). The χ -to-SSB interaction is disrupted by a single amino acid replacement near the very end of the C-terminal tail of SSB (Kelman et al., 1998), which is separated from the structural core of SSB by ~ 60 residues that are likely to be highly flexible (Raghunathan et al., 2000; Savvides et al., 2004). The specific interaction of the ψ peptide with the collar domain orients the χ : ψ heterodimer toward the emerging template strand, where it can engage the flexible tails of one or the other of the multiple SSB tetramers bound to the template strand (Figure 7C).

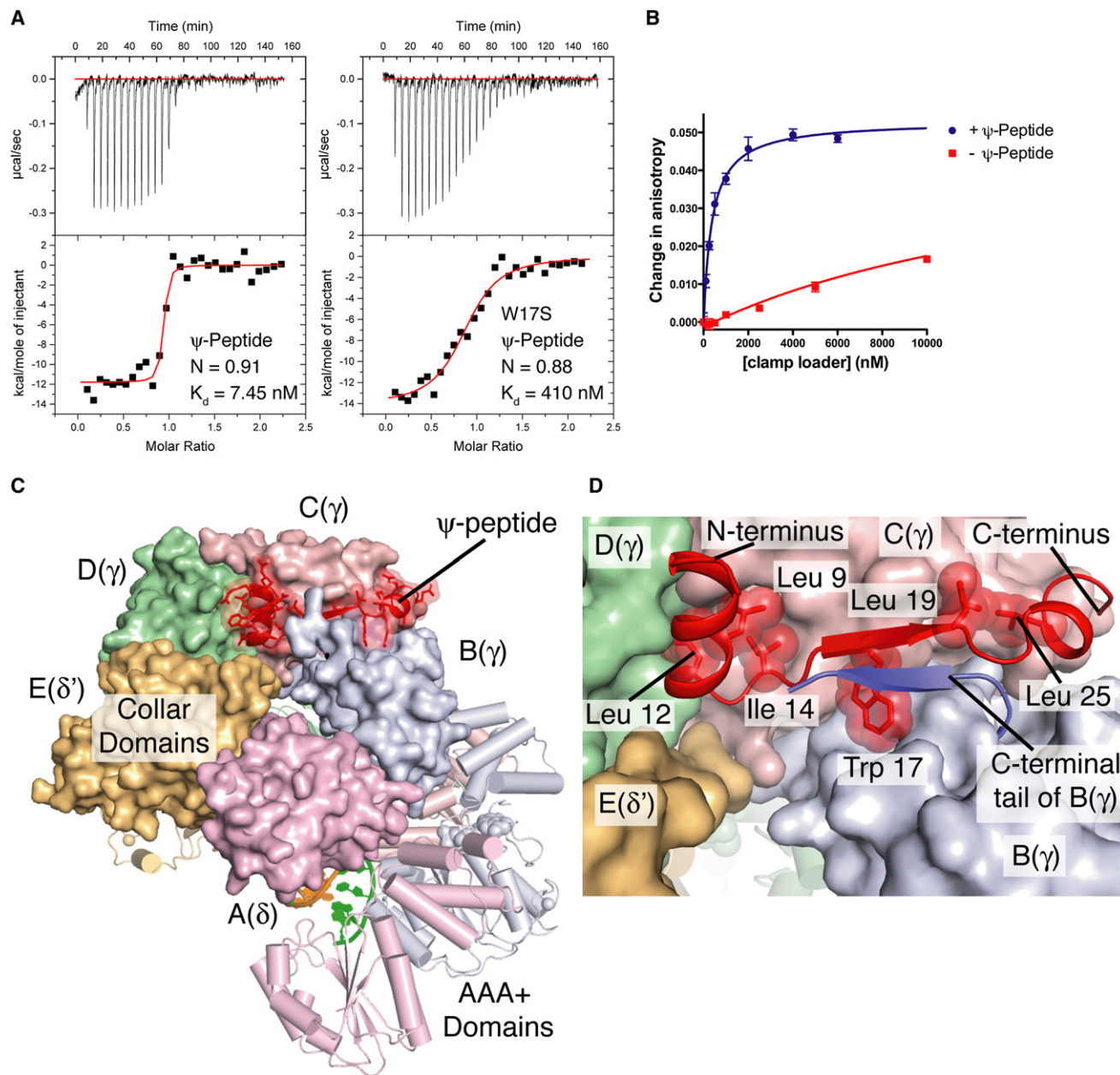


Figure 6. Binding of the ψ Peptide to the Clamp Loader Collar

(A) Isothermal titration calorimetry data for the binding of the ψ peptide to the clamp loader complex. The calorimetric titration of 100 μM wild-type ψ peptide into 10 μM of the clamp loader complex (left) and the ψ peptide with Trp 17 mutated to Ser (right) are shown. The Trp 17 mutation leads to a 55-fold decrease in binding affinity.

(B) Fluorescence anisotropy data for the binding of fluorescently labeled DNA to the clamp loader in the absence of the clamp. DNA binding in the presence (blue) and absence (red) of 10 μM ψ peptide is shown. Error bars represent the SD of individual readings. The values of the K_D of DNA binding are $0.38 \pm 0.03 \mu\text{M}$ and $18 \pm 3 \mu\text{M}$ in the presence and absence of ψ peptide, respectively.

(C) The crystal structure of the ψ peptide bound to the clamp loader collar. The clamp loader collar domains are shown as surface representations. The ψ peptide is shown in red.

(D) Close-up view of the ψ peptide interactions with the collar domains of the B(γ), C(γ), and D(γ) subunits, with hydrophobic side chains shown as spheres. The C-terminal tail of B(γ), which forms a short antiparallel β sheet with the ψ peptide, is shown as a blue ribbon.

The eukaryotic analog of SSB, replication protein-A (RP-A), is known to stimulate the loading function of RFC (Ellison and Stillman, 2003). Although there is no obvious homolog of χ : ψ in

eukaryotes, the A subunit in the eukaryotic clamp loader complex has additional domains that are not part of the clamp loader core, and one possibility is that these domains provide

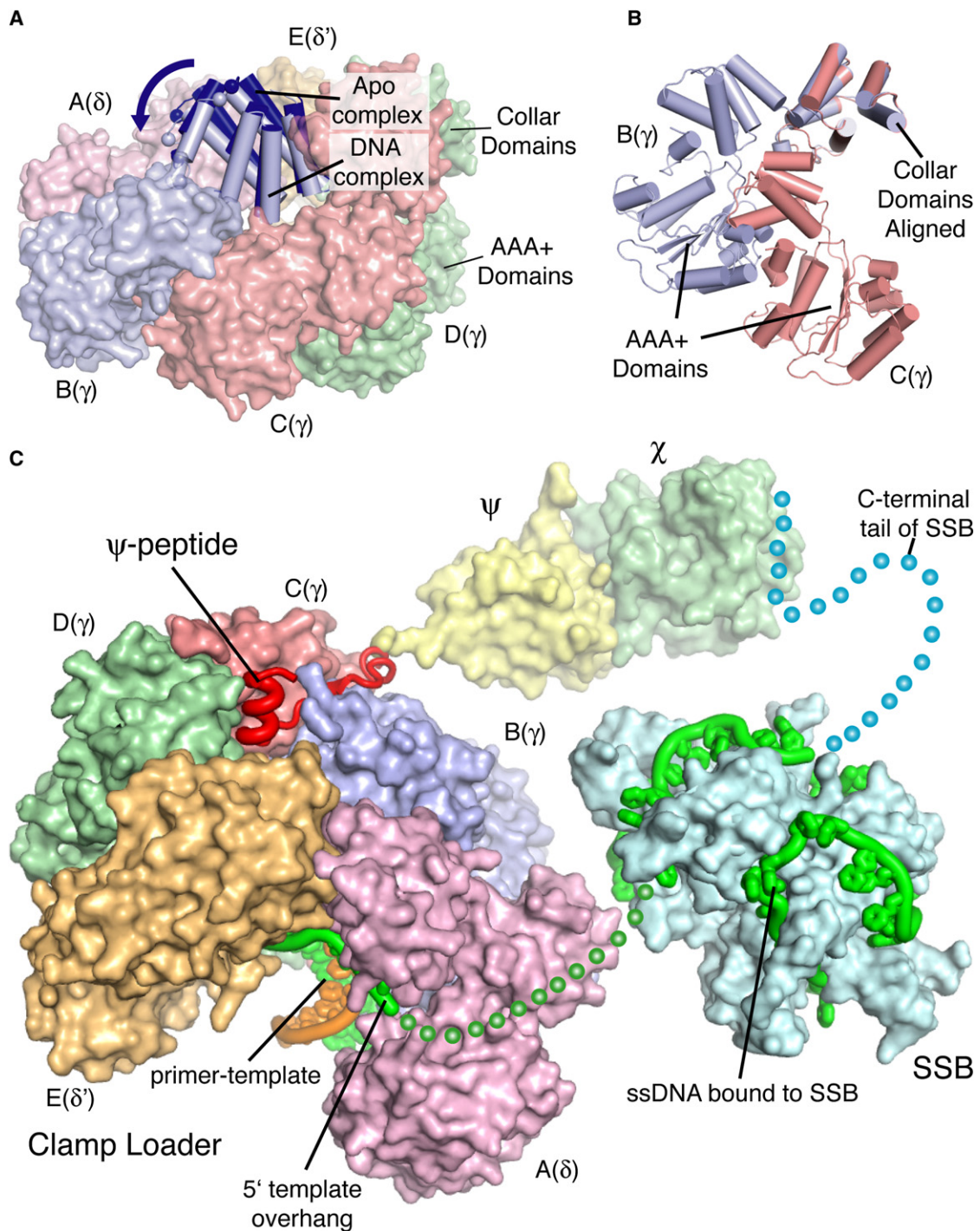


Figure 7. ψ Binding Links SSB to the Clamp Loader and Breaks Symmetry in the Collar

(A) The collar domain of the $B(\gamma)$ subunit undergoes a conformational change upon the binding of DNA by the clamp loader. Alignment of the collar domains of the apo *E. coli* clamp loader (Jeruzalmi et al., 2001a) onto the DNA-bound clamp loader reveals close overlap of the collar domains, with the exception of the $B(\gamma)$ collar domain (dark blue), which undergoes a rotation of $\sim 10^\circ$ toward the AAA+ spiral in the DNA-bound complex (shown in light blue).

(B) The collar domains of the $B(\gamma)$ and $C(\gamma)$ subunits of the DNA-bound complex are overlaid, revealing a difference in the orientation of the AAA+ domains of these subunits with respect to the collar. The AAA+ module of the B subunit (shown in light blue) rises up toward the collar domain, forming a tight interaction, whereas the C subunit (shown in red) is in an extended conformation.

(C) The location of the ψ peptide on the clamp loader positions the χ : ψ assembly for interaction with SSB bound to the single-stranded template exiting the clamp loader. The χ : ψ assembly (Gulbis et al., 2004) is positioned at the C-terminal end of the ψ peptide bound to the clamp loader. The χ subunit binds the C-terminal tail of SSB. The 5' template overhang of the DNA (green spheres) exits the clamp loader and wraps around SSB (Raghunathan et al., 2000).

a function analogous to the χ : ψ heterodimer in linking the clamp loader to RP-A.

Conclusions

Our analysis of the structure of the *E. coli* γ complex shows that, in the clamp loaders, the interfacial coordination of ATP and DNA binding results in a symmetric quaternary structure that wraps around DNA in dinucleotide steps. Critical to both specificity for 3' recessed ends and the accommodation of alternative primers is the loss in the pentameric clamp loaders of one of the six subunits of hexameric helicases. The lack of a sixth subunit allows the clamp loader to track only the template strand and avoid contact with the primer strand.

The symmetry of the ATPase domains in the DNA-bound clamp loader presents a contrast to the E1 helicase, in which the translocation of DNA is coupled to the adoption of distinct, rather than identical, conformations of the ATPase domains around the spiral (Enemark and Joshua-Tor, 2006). The primary function of ATP hydrolysis in the clamp loader is to release the complex upon the recognition of primer-template DNA (Pietroni and von Hippel, 2008), and this is accomplished by the symmetrical formation of catalytically competent ATP-binding sites. The helical arrangement adopted by the AAA+ modules represents a mismatch with the circular arrangement of the collar domains of the clamp loader, requiring that the three γ subunits position their collar domains differently with respect to each other upon DNA binding. The interaction of the ψ protein with the collar domains stabilizes this asymmetric arrangement and also sets up the clamp loader complex for interaction with SSB bound to the emerging template strand.

An insightful analysis of the T4 clamp loader system has shown recently that ATP binding to the clamp loader in the presence of the clamp, but not DNA, results in inhibition of ATPase activity and the formation of inequivalent ATP-binding sites (Pietroni and von Hippel, 2008). This inhibition is correlated with clamp opening, suggesting that the first step in the loading cycle is the formation of an ATP-bound but distorted form of the clamp loader that is specific for the open form of the clamp. DNA binding promotes ATP hydrolysis and makes the ATP-binding sites equivalent in terms of catalysis. The symmetric DNA-bound conformation that we present here is likely to represent a “departure complex” in which the clamp is closed around DNA and ATP is about to be hydrolyzed (Pietroni and von Hippel, 2008). An important issue that still requires resolution at the structural level is the nature of the coupling between ATP binding and the opening of the sliding clamp. Going beyond these details, the clamp loader complex is the central hub of the bacterial replication machinery, to which the polymerase subunits are tethered. The major challenge for the future is to understand how the clamp loader is integrated into the polymerase holoenzyme and how its action is coordinated with that of the catalytic subunits.

EXPERIMENTAL PROCEDURES

Protein Purification

Expression plasmids for the full-length, wild-type δ and δ' subunits have been described (Dong et al., 1993). Truncated γ (residues 1 to 373), either wild-type

or bearing the T157A mutation, was expressed with an N-terminal six histidine Ni^{2+} affinity tag in pET-28 (N-terminal amino acid sequence prior to the natural N terminus is MGSSHHHHHSSGLEVLFGQPH). All proteins were overexpressed in BL21 DE3 *E. coli* cells in TB media in the presence of 100 $\mu\text{g}/\text{ml}$ ampicillin (for δ and δ' proteins) or 50 $\mu\text{g}/\text{ml}$ kanamycin (for γ protein). After growth to OD_{600} of ~ 1.0 at 37°C, cells were induced to express protein by the addition of IPTG to 1 mM concentrations and incubated overnight at 18°C. Cells were frozen to -80°C for storage and lysed with a French press after thawing. Insoluble cell lysate was removed by centrifugation. Truncated wild-type and mutant (T157A) γ were purified by passage over a Ni^{2+} -NTA column. δ and δ' proteins were purified as described previously (Dong et al., 1993).

The clamp loader complex was assembled by addition of δ and δ' subunits in 1.5-fold stoichiometric excess to γ subunits with the N-terminal six histidine Ni^{2+} affinity tag still attached. The subunits were combined, and the clamp loader complex was purified by passage over a Ni^{2+} -NTA column, followed by purification over a SourceQ column, as described previously (Jeruzalmi et al., 2001a). The protein was concentrated to 100 mg/ml in 20 mM Tris (pH 7.5) and 2 mM DTT, flash frozen, and stored at -80°C . Primer-template junctions having a 10 base pair double-stranded region and either a 5 nucleotide 5' overhang (for the wild-type complex) or a 10 nucleotide overhang (mutant complex) were constructed by annealing oligonucleotides (Integrated DNA Technologies) having the sequences 5'-TTT TTT ATA GGC CAG-3' or 5'-TTT TTT TTT TTA TAG GCC AG-3' (template) and 5'-CTG GCC TAT A-3' (primer). The oligonucleotides were PAGE purified following synthesis for the wild-type clamp loader crystals. No purification was performed on the oligonucleotides used in the crystallization of the clamp loader containing the mutant (T157A) γ subunits.

Crystallization and Structure Determination

The 25 mg/ml γ complex and 150 μM primer-template DNA were incubated for 0.5 hr at room temperature in 1 mM ADP (or 1 mM ATP: γ S for the mutant clamp loader), 10 mM NaF, 2 mM BeCl_2 , 10 mM MgCl_2 , 20 mM Tris (pH 7.5), and 2 mM DTT. This protein-DNA solution was mixed in a 1:1 volume ratio in hanging drop crystal trays with a well solution of 9% PEG 400, 150 mM MgCl_2 , and 100 mM HEPES (pH 7.5) at 20°C, yielding crystals (space group P2₁2₁2₁; see Table S4) that diffract X-rays to 3.4 Å resolution for the wild-type clamp loader crystals and 3.25 Å for the mutant γ complex crystals (Tables S1 and S2).

X-ray data were collected on beamlines 8.2.1 and 8.2.2 at the Advanced Light Source (Berkeley, CA) and were processed with HKL2000 (Otwinowski and Minor, 1997). Initial phases were obtained by molecular replacement using a data set for the wild-type complex to 4.2 Å resolution using Phaser (McCoy et al., 2005) with the isolated collar domains and six copies of domain 1 of the B(γ) subunit from the structure of the apo form of the *E. coli* γ complex (Jeruzalmi et al., 2001a). Initial electron density maps allowed the placement of the remaining clamp loader domains into the model and revealed strong positive difference electron density for the phosphate groups of the DNA and for the ATP analogs. Rigid body refinement of the initial model against the 3.4 Å data set for the wild-type complex, followed by density modification using RESOLVE (Terwilliger, 2000), produced an electron density map into which the full double-stranded region of the primer-template junction and the first two bases in the 5' overhang could be built (Figure 1C). The final model (see statistics in Table S1) was refined using Phenix (Adams et al., 2002) and Coot (Emsley and Cowtan, 2004) with a single B-factor assigned to each residue. We applied noncrystallographic symmetry restraints during refinement of the structure. Each individual subunit in one clamp loader complex, as well as the bound primer-template DNA, was restrained to be similar to the corresponding molecule in the other complex. Both clamp loader complexes have essentially the same structure (rmsd in C α positions of 0.30 Å over the whole complex between assemblies in the asymmetric unit). Crystals for the mutant complex were isomorphous to those of wild-type, and refinement was initiated using the wild-type structure.

The N-terminal segment of *E. coli* ψ was synthesized as a peptide (ψ peptide, residues 2–28). The first residue in *E. coli* ψ was not included because it is not conserved. Crystals of the ψ peptide bound to the clamp loader:DNA complex were obtained by soaking the peptide into crystals obtained in the absence of peptide. Details of the crystallographic analysis of the ψ peptide cocrystallized with the apo form of the clamp loader are given in the Supplemental Data.

Activity Assays

DNA-binding and clamp loader activity assays were carried out essentially as described previously (Goedken et al., 2004, 2005). A detailed description of these assays, as well as the isothermal titration calorimetry measurements for the ψ peptide, is provided in the [Supplemental Data](#).

ACCESSION NUMBERS

Structures described here have been deposited in the Protein Data Bank with ID codes 3GLF for the clamp loader/DNA complex, 3GLG for the mutant γ T157A clamp loader/DNA complex, 3GLH for the clamp loader/ ψ peptide complex, and 3GLI for the clamp loader/ ψ peptide/DNA complex.

SUPPLEMENTAL DATA

Supplemental Data include Supplemental Results and Discussion, Supplemental Experimental Procedures, six tables, and eight figures and can be found with this article online at [http://www.cell.com/supplemental/S0092-8674\(09\)00381-X](http://www.cell.com/supplemental/S0092-8674(09)00381-X).

ACKNOWLEDGMENTS

We thank James Berger and members of the Kuriyan Lab, in particular Meindert Lamers, for helpful discussions. We are also thankful to David King for synthesis of the ψ peptide and to the staff at beamlines 8.2.1, 8.2.2, and 5.0.1 of the Advanced Light Source (Berkeley, CA) for their help and technical support. This work was supported in part by grants from the NIH to J.K. (GM45547) and M.O. (GM38839).

Received: October 13, 2008

Revised: January 22, 2009

Accepted: March 25, 2009

Published: May 14, 2009

REFERENCES

- Abrahams, J.P., Leslie, A.G., Lutter, R., and Walker, J.E. (1994). Structure at 2.8 Å resolution of F1-ATPase from bovine heart mitochondria. *Nature* 370, 621–628.
- Adams, P.D., Grosse-Kunstleve, R.W., Hung, L.W., Ioerger, T.R., McCoy, A.J., Moriarty, N.W., Read, R.J., Sacchettini, J.C., Sauter, N.K., and Terwilliger, T.C. (2002). PHENIX: Building new software for automated crystallographic structure determination. *Acta Crystallogr. D Biol. Crystallogr.* 58, 1948–1954.
- Anderson, S.G., Williams, C.R., O'Donnell, M., and Bloom, L.B. (2007). A function for the ψ subunit in loading the *Escherichia coli* DNA polymerase sliding clamp. *J. Biol. Chem.* 282, 7035–7045.
- Ason, B., Handayani, R., Williams, C.R., Bertram, J.G., Hingorani, M.M., O'Donnell, M., Goodman, M.F., and Bloom, L.B. (2003). Mechanism of loading the *Escherichia coli* DNA polymerase III beta sliding clamp on DNA. *Bona fide primer/templates preferentially trigger the gamma complex to hydrolyze ATP and load the clamp.* *J. Biol. Chem.* 278, 10033–10040.
- Benkovic, S.J., Valentine, A.M., and Salinas, F. (2001). Replisome-mediated DNA replication. *Annu. Rev. Biochem.* 70, 181–208.
- Bowman, G.D., O'Donnell, M., and Kuriyan, J. (2004). Structural analysis of a eukaryotic sliding DNA clamp-clamp loader complex. *Nature* 429, 724–730.
- Bowman, G.D., Goedken, E.R., Kazmirski, S.L., O'Donnell, M., and Kuriyan, J. (2005). DNA polymerase clamp loaders and DNA recognition. *FEBS Lett.* 579, 863–867.
- Chen, S., Coman, M.M., Sakato, M., O'Donnell, M., and Hingorani, M.M. (2008). Conserved residues in the delta subunit help the *E. coli* clamp loader, gamma complex, target primer-template DNA for clamp assembly. *Nucleic Acids Res.* 36, 3274–3286.
- Cullmann, G., Fien, K., Kobayashi, R., and Stillman, B. (1995). Characterization of the five replication factor C genes of *Saccharomyces cerevisiae*. *Mol. Cell. Biol.* 15, 4661–4671.
- Dong, Z., Onrust, R., Skangalis, M., and O'Donnell, M. (1993). DNA polymerase III accessory proteins. I. *holA* and *holB* encoding delta and delta'. *J. Biol. Chem.* 268, 11758–11765.
- Ellison, V., and Stillman, B. (2003). Biochemical characterization of DNA damage checkpoint complexes: Clamp loader and clamp complexes with specificity for 5' recessed DNA. *PLoS Biol.* 1, E33.
- Emsley, P., and Cowtan, K. (2004). Coot: Model-building tools for molecular graphics. *Acta Crystallogr. D Biol. Crystallogr.* 60, 2126–2132.
- Enemark, E.J., and Joshua-Tor, L. (2006). Mechanism of DNA translocation in a replicative hexameric helicase. *Nature* 442, 270–275.
- Fedoroff, O.Y., Salazar, M., and Reid, B.R. (1993). Structure of a DNA:RNA hybrid duplex. Why RNase H does not cleave pure RNA. *J. Mol. Biol.* 233, 509–523.
- Gao, D., and McHenry, C.S. (2001). Tau binds and organizes *Escherichia coli* replication proteins through distinct domains. Domain III, shared by gamma and tau, binds delta delta' and chi psi. *J. Biol. Chem.* 276, 4447–4453.
- Glover, B.P., and McHenry, C.S. (1998). The chi psi subunits of DNA polymerase III holoenzyme bind to single-stranded DNA-binding protein (SSB) and facilitate replication of an SSB-coated template. *J. Biol. Chem.* 273, 23476–23484.
- Goedken, E.R., Levitus, M., Johnson, A., Bustamante, C., O'Donnell, M., and Kuriyan, J. (2004). Fluorescence measurements on the *E. coli* DNA polymerase clamp loader: Implications for conformational changes during ATP and clamp binding. *J. Mol. Biol.* 336, 1047–1059.
- Goedken, E.R., Kazmirski, S.L., Bowman, G.D., O'Donnell, M., and Kuriyan, J. (2005). Mapping the interaction of DNA with the *Escherichia coli* DNA polymerase clamp loader complex. *Nat. Struct. Mol. Biol.* 12, 183–190.
- Gomes, X.V., and Burgers, P.M. (2001). ATP utilization by yeast replication factor C. I. ATP-mediated interaction with DNA and with proliferating cell nuclear antigen. *J. Biol. Chem.* 276, 34768–34775.
- Gomes, X.V., Schmidt, S.L., and Burgers, P.M. (2001). ATP utilization by yeast replication factor C. II. Multiple stepwise ATP binding events are required to load proliferating cell nuclear antigen onto primed DNA. *J. Biol. Chem.* 276, 34776–34783.
- Guenther, B., Onrust, R., Sali, A., O'Donnell, M., and Kuriyan, J. (1997). Crystal structure of the delta' subunit of the clamp-loader complex of *E. coli* DNA polymerase III. *Cell* 91, 335–345.
- Gulbis, J.M., Kazmirski, S.L., Finkelstein, J., Kelman, Z., O'Donnell, M., and Kuriyan, J. (2004). Crystal structure of the chi:psi sub-assembly of the *Escherichia coli* DNA polymerase clamp-loader complex. *Eur. J. Biochem.* 271, 439–449.
- Hattendorf, D.A., and Lindquist, S.L. (2002). Cooperative kinetics of both Hsp104 ATPase domains and interdomain communication revealed by AAA sensor-1 mutants. *EMBO J.* 21, 12–21.
- Hingorani, M.M., and O'Donnell, M. (1998). ATP binding to the *Escherichia coli* clamp loader powers opening of the ring-shaped clamp of DNA polymerase III holoenzyme. *J. Biol. Chem.* 273, 24550–24563.
- Jarvis, T.C., Beaudry, A.A., Bullard, J.M., Janjic, N., and McHenry, C.S. (2005a). Reconstitution of a minimal DNA replicase from *Pseudomonas aeruginosa* and stimulation by non-cognate auxiliary factors. *J. Biol. Chem.* 280, 7890–7900.
- Jarvis, T.C., Beaudry, A.A., Bullard, J.M., Ochsner, U., Dallmann, H.G., and McHenry, C.S. (2005b). Discovery and characterization of the cryptic psi subunit of the pseudomonad DNA replicase. *J. Biol. Chem.* 280, 40465–40473.
- Jeruzalmi, D., O'Donnell, M., and Kuriyan, J. (2001a). Crystal structure of the processivity clamp loader gamma (gamma) complex of *E. coli* DNA polymerase III. *Cell* 106, 429–441.
- Jeruzalmi, D., Yurieva, O., Zhao, Y., Young, M., Stewart, J., Hingorani, M., O'Donnell, M., and Kuriyan, J. (2001b). Mechanism of processivity clamp opening by the delta subunit wrench of the clamp loader complex of *E. coli* DNA polymerase III. *Cell* 106, 417–428.
- Johnson, A., and O'Donnell, M. (2005). Cellular DNA replicases: Components and dynamics at the replication fork. *Annu. Rev. Biochem.* 74, 283–315.

- Kazmirski, S.L., Podobnik, M., Weitze, T.F., O'Donnell, M., and Kuriyan, J. (2004). Structural analysis of the inactive state of the Escherichia coli DNA polymerase clamp-loader complex. *Proc. Natl. Acad. Sci. USA* *101*, 16750–16755.
- Kelman, Z., and White, M.F. (2005). Archaeal DNA replication and repair. *Curr. Opin. Microbiol.* *8*, 669–676.
- Kelman, Z., Yuzhakov, A., Andjelkovic, J., and O'Donnell, M. (1998). Devoted to the lagging strand—the subunit of DNA polymerase III holoenzyme contacts SSB to promote processive elongation and sliding clamp assembly. *EMBO J.* *17*, 2436–2449.
- Lahue, R.S., Au, K.G., and Modrich, P. (1989). DNA mismatch correction in a defined system. *Science* *245*, 160–164.
- Lee, J.Y., and Yang, W. (2006). UvrD helicase unwinds DNA one base pair at a time by a two-part power stroke. *Cell* *127*, 1349–1360.
- Magdalena Coman, M., Jin, M., Ceapa, R., Finkelstein, J., O'Donnell, M., Chait, B.T., and Hingorani, M.M. (2004). Dual functions, clamp opening and primer-template recognition, define a key clamp loader subunit. *J. Mol. Biol.* *342*, 1457–1469.
- McCoy, A.J., Grosse-Kunstleve, R.W., Storoni, L.C., and Read, R.J. (2005). Likelihood-enhanced fast translation functions. *Acta Crystallogr. D Biol. Crystallogr.* *61*, 458–464.
- Miyata, T., Suzuki, H., Oyama, T., Mayanagi, K., Ishino, Y., and Morikawa, K. (2005). Open clamp structure in the clamp-loading complex visualized by electron microscopic image analysis. *Proc. Natl. Acad. Sci. USA* *102*, 13795–13800.
- Naktinis, V., Onrust, R., Fang, L., and O'Donnell, M. (1995). Assembly of a chromosomal replication machine: Two DNA polymerases, a clamp loader, and sliding clamps in one holoenzyme particle. II. Intermediate complex between the clamp loader and its clamp. *J. Biol. Chem.* *270*, 13358–13365.
- Neuwald, A.F., Aravind, L., Spouge, J.L., and Koonin, E.V. (1999). AAA+: A class of chaperone-like ATPases associated with the assembly, operation, and disassembly of protein complexes. *Genome Res.* *9*, 27–43.
- Nowotny, M., Gaidamakov, S.A., Crouch, R.J., and Yang, W. (2005). Crystal structures of RNase H bound to an RNA/DNA hybrid: Substrate specificity and metal-dependent catalysis. *Cell* *121*, 1005–1016.
- O'Donnell, M., Onrust, R., Dean, F.B., Chen, M., and Hurwitz, J. (1993). Homology in accessory proteins of replicative polymerases—E. coli to humans. *Nucleic Acids Res.* *21*, 1–3.
- Olson, M.W., Dallmann, H.G., and McHenry, C.S. (1995). DnaX complex of Escherichia coli DNA polymerase III holoenzyme. The chi psi complex functions by increasing the affinity of tau and gamma for delta.delta' to a physiologically relevant range. *J. Biol. Chem.* *270*, 29570–29577.
- Otwinowski, Z., and Minor, W. (1997). Processing of X-ray diffraction data collected in oscillation mode. *Methods Enzymol.* *276*, 307–326.
- Oyama, T., Ishino, Y., Cann, I.K., Ishino, S., and Morikawa, K. (2001). Atomic structure of the clamp loader small subunit from Pyrococcus furiosus. *Mol. Cell* *8*, 455–463.
- Ozawa, K., Jergic, S., Crowther, J.A., Thompson, P.R., Wijffels, G., Otting, G., and Dixon, N.A. (2005). Cell-free protein synthesis in an autoinduction system for NMR studies of protein-protein interactions. *J. Biomol. NMR* *32*, 235–241.
- Pietroni, P., and von Hippel, P.H. (2008). Multiple ATP binding is required to stabilize the “activated” (clamp open) clamp loader of the T4 DNA replication complex. *J. Biol. Chem.* *283*, 28338–28353.
- Raghunathan, S., Kozlov, A.G., Lohman, T.M., and Waksman, G. (2000). Structure of the DNA binding domain of E. coli SSB bound to ssDNA. *Nat. Struct. Biol.* *7*, 648–652.
- Savvides, S.N., Raghunathan, S., Futterer, K., Kozlov, A.G., Lohman, T.M., and Waksman, G. (2004). The C-terminal domain of full-length E. coli SSB is disordered even when bound to DNA. *Protein Sci.* *13*, 1942–1947.
- Skordalakes, E., and Berger, J.M. (2006). Structural insights into RNA-dependent ring closure and ATPase activation by the Rho termination factor. *Cell* *127*, 553–564.
- Terwilliger, T.C. (2000). Maximum-likelihood density modification. *Acta Crystallogr. D Biol. Crystallogr.* *56*, 965–972.
- Waga, S., and Stillman, B. (1998). The DNA replication fork in eukaryotic cells. *Annu. Rev. Biochem.* *67*, 721–751.
- Witte, G., Urbanke, C., and Curth, U. (2003). DNA polymerase III chi subunit ties single-stranded DNA binding protein to the bacterial replication machinery. *Nucleic Acids Res.* *31*, 4434–4440.
- Yao, N.Y., Johnson, A., Bowman, G.D., Kuriyan, J., and O'Donnell, M. (2006). Mechanism of proliferating cell nuclear antigen clamp opening by replication factor C. *J. Biol. Chem.* *281*, 17528–17539.
- Yuzhakov, A., Kelman, Z., and O'Donnell, M. (1999). Trading places on DNA—A three-point switch underlies primer handoff from primase to the replicative DNA polymerase. *Cell* *96*, 153–163.
- Zhuang, Z., Berdis, A.J., and Benkovic, S.J. (2006a). An alternative clamp loading pathway via the T4 clamp loader gp44/62-DNA complex. *Biochemistry* *45*, 7976–7989.
- Zhuang, Z., Yoder, B.L., Burgers, P.M., and Benkovic, S.J. (2006b). The structure of a ring-opened proliferating cell nuclear antigen-replication factor C complex revealed by fluorescence energy transfer. *Proc. Natl. Acad. Sci. USA* *103*, 2546–2551.